



Published in final edited form as:

*Biomaterials*. 2010 January ; 31(1): 1–8. doi:10.1016/j.biomaterials.2009.09.025.

## ***In situ* elasticity modulation with dynamic substrates to direct cell phenotype**

April M. Kloxin<sup>1</sup>, Julie A. Benton<sup>1,+</sup>, and Kristi S. Anseth<sup>1,2,\*</sup>

<sup>1</sup>Department of Chemical and Biological Engineering, University of Colorado, 424 UCB, ECCH 111, Boulder, CO 80309 USA, Department Phone: 303.492.7471, Fax: 303.735.0095

<sup>2</sup>Howard Hughes Medical Institute, University of Colorado, 424 UCB, ECCH 111, Boulder, CO 80309 USA, Department Phone: 303.492.7471, Fax: 303.735.0095

### **Abstract**

Microenvironment elasticity influences critical cell functions such as differentiation, cytoskeletal organization, and process extension. Unfortunately, few materials allow elasticity modulation in real-time to probe its direct effect on these dynamic cellular processes. Here, a new approach is presented for the photochemical modulation of elasticity within the cell's microenvironment at any point in time. A photodegradable hydrogel was irradiated and degraded under cytocompatible conditions to generate a wide range of elastic moduli similar to soft tissues and characterized using rheometry and atomic force microscopy (AFM). The effect of the elastic modulus on valvular interstitial cell (VIC) activation into myofibroblasts was explored. In these studies, gradient samples were used to identify moduli that either promote or suppress VIC myofibroblastic activation. With this knowledge, VICs were cultured on a high modulus, activating hydrogel substrate, and uniquely, results show that decreasing the substrate modulus with irradiation reverses this activation, demonstrating that myofibroblasts can be de-activated solely by changing the modulus of the underlying substrate. This finding is important for the rational design of biomaterials for tissue regeneration and offers insight into fibrotic disease progression. These photodegradable hydrogels demonstrate the capability to both probe and direct cell function through dynamic changes in substrate elasticity.

### **1. Introduction**

Fabrication of cell culture substrates with different elastic moduli has been explored for the past decade, as researchers identified that cell contractile forces and related cell functions, such as motility [1], cytoskeletal organization [2], and differentiation [3,4], are influenced by the elasticity of the underlying substrate [5,6]. For example, in response to an injury, fibroblasts are known to differentiate into myofibroblasts, a wound healing phenotype responsible for repairing and replacing damaged extracellular matrix (ECM) in injured tissues and organs [7]. As ECM is secreted, the elastic modulus of the cell microenvironment increases. Once the desired matrix modulus is achieved, the myofibroblasts deactivate and undergo a number of cellular processes, including senescence [8] and apoptosis [7], the exact pathways of which

\*Author to whom correspondence should be addressed: Kristi.Anseth@colorado.edu.

<sup>+</sup>Current address: Edwards Lifesciences, HVT Research & Development, One Edwards Way, Irvine, CA 92614

**Appendix:** Supplementary data associated with this article can be found online. Certain parts of the figures may be difficult to interpret in black and white. The full colour images can be found in the online version.

**Publisher's Disclaimer:** This is a PDF file of an unedited manuscript that has been accepted for publication. As a service to our customers we are providing this early version of the manuscript. The manuscript will undergo copyediting, typesetting, and review of the resulting proof before it is published in its final citable form. Please note that during the production process errors may be discovered which could affect the content, and all legal disclaimers that apply to the journal pertain.

are not well understood. If this deactivation is misregulated and the myofibroblast phenotype persists, ECM secretion continues, increasing the matrix modulus and effecting fibrosis [9]. Understanding the role of the matrix modulus in dynamic cellular signaling processes such as these is important for treatment of fibrotic diseases, as well as in the design of tissue regeneration strategies [3]. Many researchers have thus sought to explore the influence of substrate elasticity on cell function by the development of materials with highly regulated properties.

Researchers have used discrete poly(acrylamide)-, poly(ethylene glycol) (PEG)-, or poly(dimethyl siloxane)-based gels with different moduli to explore cellular processes such as myotube differentiation [10], embryonic cardiomyocyte beating [11], and neuronal cell process extension [12]; smooth muscle cell (SMC) proliferation and focal adhesion formation [13]; and myofibroblastic activation [14], respectively. These materials are useful but require the preparation of a unique formulation for each gel (e.g., different crosslinker concentration) to vary the modulus, and more importantly, the material properties are fixed upon formation. To address some of these limitations, advanced processing techniques have been developed to create modulus gradients within hydrogels [15,16]. For example, gradient hydrogels formed from mixtures of acrylamide and bis-acrylamide have been used to study fibroblast migration [17]. Improved gradient fabrication techniques, such as using microfluidics with poly(acrylamide)-hydrogels [18] and advanced patterning with poly(dimethylsiloxane) (PDMS) [19] gels, have been used to examine vascular SMC spreading and cytoskeletal organization [18] and fibroblast and endothelial cell migration [19], respectively. While these approaches have been proven versatile, the material properties are static. Recently, Frey and Wang developed a polyacrylamide-based photodegradable hydrogel whose modulus can be decreased 20-30% of its initial value with irradiation in the presence of NIH 3T3 fibroblasts [20]. This dynamic modulation of substrate rigidity was used to study the influence of modulus on 3T3 cell morphology and migration. In parallel to this work, we were interested in probing the influence of dynamic changes in substrate modulus on cell function (e.g., differentiation), which often requires a large variation in modulus. Specifically, we have developed a photodegradable monomer for synthesizing PEG-based hydrogels that degrade in response to light, and the chemistry is compatible with cell encapsulation and 3D cell culture [21]. Here, we exploit this chemistry to create a 2D cell culture platform whose elasticity can be tuned over a wide range of moduli and subsequently varied in real-time by exposure to light. Experiments were designed to answer how *in situ* changes in substrate modulus might influence the fibroblast-myofibroblast differentiation process, especially how myofibroblast de-differentiation might be directed by a step change in the elasticity of its microenvironment. In general, a cell culture substrate that allows on-demand creation of materials with variable elasticity, either in a discrete or gradient fashion, would allow the design of unique experiments to further explore the influence of elasticity on cellular functions. Moreover, such materials would improve the understanding of how cells respond to dynamic microenvironmental changes (e.g., the role of matrix elasticity in promoting or suppressing fibrosis).

## 2. Materials and Methods

### 2.1. Hydrogel preparation

The photodegradable crosslinker (PEGdiPDA) was synthesized as previously described [22]. PEGdiPDA ( $M_n \sim 4070$  g/mol, 8.2 wt%) was copolymerized with PEGA ( $M_n \sim 400$  g/mol, 6.8 wt%, Monomer-Polymer and Dajac Laboratories, Inc) in PBS via redox-initiated free radical polymerization using 0.2 M ammonium persulfate (AP) and subsequently adding 0.1 M tetraethylmethylenediamine (TEMED) while vortexing. The polymerization is complete within 5 min, based on modulus evolution followed by rheometry. The hydrogels were formed *in situ* for rheometry experiments. For all other experiments, hydrogels were polymerized

between glass coverslips (22 mm × 22 mm) separated by a 0.25-mm thick spacer (9 mm × 9 mm). For cell experiments, fibronectin (100 nM, BD Bioscience) was mixed in the monomer solution and entrapped within the hydrogel. Uniform presentation of fibronectin with degradation was verified by fluorescent labeling of the protein and subsequent imaging *in situ* (Supplemental Figure S1). The hydrogel was covalently linked to one of the coverslips during polymerization by methacrylation of the coverslip directly prior to use. The methacrylated coverslip was prepared by cleaning of the slip with Piranha (30 min, 3:1 by volume sulfuric acid:hydrogen peroxide), rinsing with copious amounts of deionized (DI) water, rinsing with acetone, and chemical vapor deposition of methacrylopropyltrimethoxysilane (Gelest) at 60°C for 3 h under argon. After preparation, hydrogels were transferred to PBS for AFM characterization or to cell culture media (M199, Invitrogen) with 1 µg/mL amphotericin B, 50 U/mL penicillin, and 50 µg/mL streptomycin. Media was refreshed after 12 h to remove any remaining monomer or initiator.

## 2.2. Hydrogel characterization with rheometry

Hydrogel degradation was characterized with a photorheometer ( $\gamma = 10\%$ ,  $\omega = 10$  rad/s for linear viscoelastic regime, ARES, TA). A thin hydrogel film (0.05 mm) was polymerized *in situ* between an 8 mm diameter flat quartz plate and a temperature-controlled Peltier flat plate (25°C). Upon complete polymerization, the hydrogel was surrounded with a small amount of water to prevent dehydration, and the hydrogel storage modulus ( $G'$ ) was monitored, which dominates for these elastic polymer networks ( $G \approx G'$  when  $G' > G''$ ) [23], while irradiating the sample with UV light (365 nm at 10 mW/cm<sup>2</sup>, EXFO, Novacure, high-pressure mercury arc lamp with light guide and collimating lens). To follow degradation,  $G'$  was normalized to its initial value  $G'_0$ . The storage modulus was converted to Young's modulus ( $E$ ) using rubber

elasticity theory, where  $G = \frac{E}{2(1+\nu)}$ , assuming a Poisson's ratio ( $\nu$ ) of 0.5 for bulk measurements of elastic hydrogel polymer networks [23,24].

## 2.3. Hydrogel film degradation and characterization with AFM

A surface elasticity gradient was created by irradiating the surface of a photodegradable hydrogel with a light gradient (365 nm at 10 mW/cm<sup>2</sup> for 0 to 5 min across the surface, where light penetration and gel degradation are limited to the top ~ 50 µm of the gel). This light gradient was achieved by irradiating the hydrogel while continuously covering the hydrogel surface with an opaque plate from one side (0 mm) to another (9 mm) with a cover plate attached to a linear motion stage [25]. The covering rate is set so that the entire sample was covered prior to complete degradation of the sample surface (< 10 min of 365 nm at 10 mW/cm<sup>2</sup> as determined by rheometry). This degradation gradient creates a gradient in surface elasticity from the initial hydrogel modulus on one side of the gel to a modulus that is ~ 20% of the initial value after 5 min of degradation on the other side of the gel. The resulting surface elasticity gradient was measured with atomic force microscopy [26] (AFM, PicoPlus<sup>TM</sup> scanning probe microscope, Molecular Imaging, Inc., pyramidal silicon nitride tip with force constant 0.12 N/m, radius = 10 nm, height = 2.5 - 3.5 nm, and angle of pyramid = 35°), where  $E$  at various linear positions across a gel surface was obtained using the Hertz model and  $\nu \approx 0.2$  for the surface of a PEG hydrogel [27]. Discrete samples with high and low moduli were similarly prepared except with either no irradiation or flood irradiation of the entire sample for 5 min (365 nm at 10 mW/cm<sup>2</sup>). In addition, elasticity was modulated in the presence of cells on discrete, high modulus samples with flood irradiation for 5 min (365 nm at 10 mW/cm<sup>2</sup>).

## 2.4. Cell culture

VICs were isolated from porcine aortic valve leaflets by sequential collagenase digestion as previously described within 24 hours after sacrifice [28]. Isolated cells were cultured in growth

media (Medium 199, 15% fetal bovine serum (FBS), 2% penicillin/streptomycin (100 U/mL), 0.4% fungizone (0.5  $\mu\text{g/mL}$ )) and successively passaged (passage 2 and 3 used for experiments). All experiments were performed in low serum (1% FBS supplemented) media to minimize cell proliferation and plated at 40,000 cells/cm<sup>2</sup>.

## 2.5. Real-time cell tracking

Time lapse images of cell movement were captured every 15 min over a 3 day period using a Nikon TE 2000 PFS fluorescent microscope equipped with a motorized stage and an environmental sample chamber. Images were collected and analyzed using MetaMorph software (Molecular Devices). Velocities were calculated by taking the change in cell position divided by the time interval (i.e., 15 min) over 3 days, which were subsequently averaged for each cell. The velocities presented are average velocities for several cells over 3 days on the gradient substrates.

## 2.6. Immunostaining

Samples were fixed with 10% buffered formalin, permeabilized in 0.05 wt% Tween 20, blocked with 3 wt% bovine serum albumin (BSA), and incubated with mouse anti- $\alpha$ -smooth muscle actin ( $\alpha$ SMA) (Abcam) antibody. Following primary antibody coupling, samples were washed and incubated with goat-anti-mouse Alexa 488 (Invitrogen) and phalloidin-tetramethylrhodamine B isothiocyanate (Sigma-Aldrich). Samples were subsequently counterstained with DAPI and imaged on a Nikon TE 2000 epi-fluorescence microscope with 20 $\times$  magnification objective. Images from each fluorescent channel were merged, and the background was flattened using MetaMorph. The number of cells was counted using the DAPI channel and ImageJ (Analyze Particles function, NIH). The number of myofibroblasts were counted manually by identifying cells with  $\alpha$ SMA organized into fibrils, and the percentage of myofibroblasts was calculated by dividing the number of myofibroblasts by the total number cells and multiplying by 100%.

## 2.7. Gene expression

Cells were transfected with a  $\alpha$ SMA-luciferase reporter construct (5  $\mu\text{g}$  plasmid), developed by N.A. Rice [29], using an Amaxa Nucleofector (program U-23 as recommended by the manufacturer). Cells were then seeded on hydrogels, and samples were analyzed for luciferase activity on Day 1 and 3 (Promega Bright-Glo Luciferase Assay System per manufacturers instructions).

## 2.8. Statistics

All data collected are presented as mean  $\pm$  standard error of three or more samples. A Student's t-test was used to compare data sets, and the resulting  $p$  values that were used to determine statistical significance are noted.

# 3. Results and Discussion

## 3.1. Synthesis of photodegradable hydrogels and tuning of their mechanical properties with irradiation

Valvular interstitial cell (VIC) activation to myofibroblasts has been linked to fibrotic valve disease [30]. Further, the fibroblast-to-myofibroblast transition is important in numerous wound healing processes and has been linked to several disease states [7]. To investigate the influence of *in situ* substrate modulus variation on VIC culture and myofibroblastic activation, we synthesized hydrogel films by copolymerizing a photodegradable PEG diacrylate crosslinking macromer (PEGdiPDA) [21] with PEG monoacrylate (PEGA) in phosphate buffered saline (PBS) (Figure 1a). Bulk degradation of these hydrogels under cytocompatible

irradiation conditions [31] was characterized with rheometry. Thin films were polymerized and subsequently uniformly irradiated while monitoring changes in the hydrogel storage modulus ( $G'$ ). As the hydrogel degrades,  $G'$ , which is directly proportional to the crosslinking density, decreases (plot, Figure 1b). With continuous irradiation, the thin film undergoes reverse gelation within 10 minutes. Prior to this, degradation is arrested by ceasing irradiation [22]. Hydrogel elasticity thus can be tailored spatially and temporally via the control of irradiation.

The photodegradable hydrogels were thus used to examine the influence of the substrate elasticity on fibroblast activation, specifically, VIC differentiation into myofibroblasts (images, Figure 1b). The myofibroblast phenotype, which is up-regulated upon valve injury, demonstrates unique wound healing functions such as producing significant amounts of ECM for tissue regeneration. However, myofibroblast persistence is associated with the development of fibrotic pathologies including valvular stenosis [30, 32-34], a degenerative hardening of the valve [35] characterized by a change from an elastic, pliable tissue to a stiff, calcified tissue [36]. Myofibroblasts possess qualities of fibroblasts and of SMCs, with an intricate cytoskeleton dominated by  $\alpha$ -smooth muscle actin ( $\alpha$ SMA) positive stress fibers [37]. In response to stimuli such as exposure to the growth factor TGF- $\beta_1$  [38] or *in vitro* cell culture on stiff substrates [39], the VIC population begins to differentiate, exhibiting an increased myofibroblast presence as indicated by *de novo*  $\alpha$ SMA production and organization into stress fibers. Controlling this VIC differentiation into myofibroblasts has significant implications for the improvement of strategies to treat valve disease or regenerate healthy leaflets; however, this differentiation in response to microenvironment stiffness remains poorly understood. To date, a substrate able to prevent VIC differentiation based on its modulus has yet to be identified (Figure 1b), and thus gradient modulus substrates were first used to screen the influence of a range of moduli on VIC phenotype.

### 3.2. Substrates with a gradient in modulus created by hydrogel photodegradation

A hydrogel elastic modulus gradient was induced in a photodegradable hydrogel film by moving an opaque platform across the surface during irradiation [25]. Thus, the hydrogel film was continuously covered from left to right, creating a linear exposure gradient across its surface (Figure 2a). The resulting modulus gradient was characterized by AFM [26,27], and the observed elastic moduli at discrete points across the surface compared well with rheometry measurements at corresponding irradiation times (Figure 2b). The elastic modulus varies continuously across the surface, ranging from an initial, non-irradiated value of  $\sim 32$  kPa (at 0 mm) to a final value of  $\sim 7$  kPa (at 9 mm) after 5 min of irradiation. With this approach, the hydrogel modulus was controlled post-polymerization via irradiation to create a gradient that spans the modulus range of soft tissues, from collagenous bone to muscle [4].

### 3.3. Cell migration on gradient moduli samples was insignificant

VICs were cultured on the modulus gradient hydrogels to examine the influence of substrate moduli on VIC myofibroblastic activation. Cell adhesion was promoted by entrapment of the adhesive ECM protein fibronectin into the hydrogel matrix. To avoid migration via mechanotaxis, a shallow modulus gradient across the surface was created ( $\sim 3$  kPa/mm), minimizing the modulus variation across an individual cell body ( $\sim 0.03$  kPa over  $10 \mu\text{m}$  as compared to  $\sim 1.6$  kPa over  $10 \mu\text{m}$ , where migration has been observed with 3T3 fibroblasts [17]) and focusing the study on cell activation rather than migration. While this approach may limit migration, vascular smooth cell mechanotaxis has been observed on a similar modulus steepness ( $\sim 0.94$  kPa/mm) with polyacrylamide gradient moduli hydrogels [1]. To verify that VIC migration was insignificant on the gradient substrates presented here, cells were tracked by real-time imaging at discrete positions across the gradient (32, 15, and 7 kPa) over 3 days. The average x- and y-direction velocities of the tracked cells were statistically the same and



include 0  $\mu\text{m}/\text{min}$ , indicating that the cells were not migrating in any specific direction (Figure 3). Although no significant directional migration was observed under these conditions, a steeper hydrogel elasticity gradient [17], which can be easily achieved with these photodegradable substrates, might encourage cell migration and be useful for exploring this cellular process.

### **3.4. Substrate moduli for promoting or suppressing myofibroblastic differentiation elucidated with gradient moduli hydrogels and confirmed with discrete modulus hydrogels**

VIC differentiation into myofibroblasts was examined with immunostaining for  $\alpha\text{SMA}$ , which, when organized into fibrils, is a conclusive indicator of myofibroblasts [7]. Initially, the  $\alpha\text{SMA}$  concentration was diffuse and slightly higher on the high-modulus region of the hydrogel (i.e., non-irradiated region,  $E \sim 32$  kPa) (Figure 4a). By Day 3,  $\alpha\text{SMA}$  stress fibers were pronounced on the high-modulus region, indicating significant myofibroblastic differentiation. Conversely, on the low-modulus region of the hydrogel ( $E \sim 7$  kPa),  $\alpha\text{SMA}$  was initially diffuse on Day 1 and, by Day 3, no longer observed. The percentage of myofibroblasts was quantified at representative positions, and a decrease in cell activation was observed along the gradient, with a minimum value on the low-modulus region of the hydrogel (Figure 4b). A modulus threshold for VIC activation around 15 kPa was identified with these gradient modulus hydrogels, establishing a modulus above or below which myofibroblastic activation could be either induced or prevented.

To verify that the two modulus extremes individually promote or suppress VIC differentiation, uniform samples of high (32 kPa) and low modulus (7 kPa) were prepared. Modest  $\alpha\text{SMA}$  expression was observed on both substrates over the first two days, but a marked increase in  $\alpha\text{SMA}$  stress fibers was observed on the high modulus substrates by Day 3 (Figure 5a), confirming the initial gradient screening conclusion that low modulus substrates limit VIC activation. Moreover,  $\alpha\text{SMA}$  transcriptional up-regulation was confirmed by a firefly luciferase-driven  $\alpha\text{SMA}$  gene expression reporter assay, which indicates up-regulation of  $\alpha\text{SMA}$  on high-versus low-modulus substrates on both Day 1 and 3 (Figure 5b). Thus, a substrate modulus similar to that of collagenous bone [4] promotes VIC myofibroblastic differentiation, while a modulus similar to that of muscle [4] suppresses this differentiation. This finding allows further insight into the progression of valve fibrosis. During disease progression, fibrotic valves become increasingly stiff in response to aberrant matrix accumulation; while the initial insults resulting in fibrosis are unclear, increases in matrix stiffness may lead to a feedback mechanism that accelerates the rate of progression of fibrosis, eventually leading to sclerotic and stenotic pathologies. Similar myofibroblastic responses to substrate modulus from resident fibroblast cells have been observed in dermal tissue [7], but what remains unclear is what happens to myofibroblast fate when the matrix modulus is relaxed. Answering this question requires the culture of cells on substrates with moduli that can be dynamically changed during the experiment.

### **3.5. In situ tuning of substrate modulus induces myofibroblastic de-activation**

The uniqueness of the photodegradable chemistry enables modification of the substrate modulus in the presence of cells, which allows one to explore the effect of dynamic modulus variation on VIC activation. VICs were cultured on uniform hydrogels of either high or low modulus (32 or 7 kPa) for 5 days (Figure 6a and 6b). On Day 3, a portion of the high modulus samples, where the VICs had been activated (see Figure 5), was irradiated to partially degrade the material and decrease its modulus (from 32 to 7 kPa). Upon this *in situ* decrease in modulus, cytoskeletal reorganization and cell de-activation were observed by Day 5 (Figure 6c). Here,  $\alpha\text{SMA}$  was not observed in the cytoskeleton, indicating VIC de-activation from the myofibroblast phenotype; it should be noted that cell number and viability were unaffected by the irradiation or modulus change (Supplemental Figure S2), indicating that the de-activated

cells do not immediately undergo apoptosis. In addition, cell differentiation and viability did not change with exposure to gel degradation products and light in control experiments (Supplemental Figure S3), confirming that cell de-activation was exclusively initiated by decreasing the modulus of the underlying substrate. To our knowledge, this is the first study showing myofibroblastic de-activation in response to a substrate mechanical stimulus. This finding can be used in the design of materials for valve regeneration and furthers understanding of how substrate modulus regulates the fibroblast-to-myofibroblast transition. In future experimentation, these photodegradable substrates should prove useful in long-term culture to elucidate the fate of these de-activated cells or to explore the influence of dynamic microenvironment elasticity on other cell types or functions.

## 4. Conclusions

In sum, photodegradable hydrogel films were degraded under cytocompatible irradiation conditions to create substrates with a discrete or gradient modulus from a single hydrogel composition. The gradient substrates were used to screen the influence of microenvironment elasticity on cell differentiation without influencing cell migration, identifying high and low moduli that promoted or suppressed VIC myofibroblastic differentiation. Finally, the influence of dynamic changes in the elasticity on VIC fibroblast-to-myofibroblast activation was examined by irradiating samples with activated cells, decreasing the modulus and inducing cell de-activation. A new platform for the control of substrate modulus has been created and may prove useful for further exploration of mechanotransduction and its effect on cell differentiation and migration for understanding their role in disease and tissue regeneration.

## Supplementary Material

Refer to Web version on PubMed Central for supplementary material.

## Acknowledgments

The authors thank Dr. Nancy A. Rice (Western Kentucky University) and Dr. Leslie A. Leinwand (University of Colorado at Boulder) for providing the  $\alpha$ SMA-luciferase plasmid. The authors thank Mrs. Abigail L. Bernard and Dr. Vaibhav S. Khire for AFM assistance, Dr. Christopher J. Kloxin for rheometer assistance, and Dr. Christopher N. Bowman for use of the AFM and rheometer. The authors thank Dr. Peter D. Mariner, Dr. Timothy F. Scott, and Dr. Christopher J. Kloxin for feedback on earlier versions of this manuscript. The authors thank the NIH (HL089260) and HHMI for funding this work, NASA GSRP and DoEd GAANN fellowships for AMK, and NSF GRFP and DoEd GAANN fellowships for JAB.

## References

1. Wong JY, Velasco A, Rajagopalan P, Pham Q. Directed movement of vascular smooth muscle cells on gradient-compliant hydrogels. *Langmuir* 2003;19:1908–13.
2. Peyton SR, Ghajar CM, Khatiwala CB, Putnam AJ. The emergence of ECM mechanics and cytoskeletal tension as important regulators of cell function. *Cell Biochem Biophys* 2007;47:300–20. [PubMed: 17652777]
3. Discher DE, Janmey P, Wang YL. Tissue cells feel and respond to the stiffness of their substrate. *Science* 2005;310:1139–43. [PubMed: 16293750]
4. Engler AJ, Sen S, Sweeney HL, Discher DE. Matrix elasticity directs stem cell lineage specification. *Cell* 2006;126:677–89. [PubMed: 16923388]
5. Pelham RJ, Wang YL. Cell locomotion and focal adhesions are regulated by substrate flexibility. *Proc Natl Acad Sci U S A* 1997;94:13661–5. [PubMed: 9391082]
6. Chen CS. Mechanotransduction - a field pulling together? *J Cell Sci* 2008;121:3285–92. [PubMed: 18843115]
7. Hinz B. Formation and function of the myofibroblast during tissue repair. *J Invest Dermatol* 2007;127:526–37. [PubMed: 17299435]

8. Krizhanovsky V, Yon M, Dickins RA, Hearn S, Simon J, Miething C, et al. Senescence of activated stellate cells limits liver fibrosis. *Cell* 2008;134:657–67. [PubMed: 18724938]
9. Wells RG. The role of matrix stiffness in regulating cell behavior. *Hepatology* 2008;47:1394–400. [PubMed: 18307210]
10. Engler AJ, Griffin MA, Sen S, Bonnetmann CG, Sweeney HL, Discher DE. Myotubes differentiate optimally on substrates with tissue-like stiffness: pathological implications for soft or stiff microenvironments. *J Cell Biol* 2004;166:877–87. [PubMed: 15364962]
11. Engler AJ, Carag-Krieger C, Johnson CP, Raab M, Tang HY, Speicher DW, et al. Embryonic cardiomyocytes beat best on a matrix with heart-like elasticity: scar-like rigidity inhibits beating. *J Cell Sci* 2008;121:3794–802. [PubMed: 18957515]
12. Leach JB, Brown XQ, Jacot JG, DiMilla PA, Wong JY. Neurite outgrowth and branching of PC12 cells on very soft substrates sharply decreases below a threshold of substrate rigidity. *J Neural Eng* 2007;4:26–34. [PubMed: 17409477]
13. Peyton SR, Raub CB, Keschrums VP, Putnam AJ. The use of poly(ethylene glycol) hydrogels to investigate the impact of ECM chemistry and mechanics on smooth muscle cells. *Biomaterials* 2006;27:4881–93. [PubMed: 16762407]
14. Wipff PJ, Rifkin DB, Meister JJ, Hinz B. Myofibroblast contraction activates latent TGF-beta 1 from the extracellular matrix. *J Cell Biol* 2007;179:1311–23. [PubMed: 18086923]
15. Maskarinec SA, Tirrell DA. Protein engineering approaches to biomaterials design. *Curr Opin Biotechnol* 2005;16:422–6. [PubMed: 16006115]
16. Genzer J, Bhat RR. Surface-bound soft matter gradients. *Langmuir* 2008;24:2294–317. [PubMed: 18220435]
17. Lo CM, Wang HB, Dembo M, Wang YL. Cell movement is guided by the rigidity of the substrate. *Biophys J* 2000;79:144–52. [PubMed: 10866943]
18. Zaari N, Rajagopalan P, Kim SK, Engler AJ, Wong JY. Photopolymerization in microfluidic gradient generators: Microscale control of substrate compliance to manipulate cell response. *Adv Mater* 2004;16:2133–7.
19. Gray DS, Tien J, Chen CS. Repositioning of cells by mechanotaxis on surfaces with micropatterned Young's modulus. *J Biomed Mater Res Part A* 2003;66A:605–14.
20. Frey MT, Wang YL. A photo-modulatable material for probing cellular responses to substrate rigidity. *Soft Matter* 2009;5:1918–24. [PubMed: 19672325]
21. Kloxin AM, Kasko AM, Salinas CN, Anseth KS. Photodegradable Hydrogels for Dynamic Tuning of Physical and Chemical Properties. *Science* 2009;324:59–63. [PubMed: 19342581]
22. Kloxin AM, Kasko AM, Salinas CN, Anseth KS. Photodegradable hydrogels for dynamic tuning of physical and chemical properties. *Science*. 2009Accepted
23. Young, RJ.; Lovell, PA. Introduction to polymers. Vol. 2nd. London, U. K.: Chapman & Hall; 1991.
24. Bryant, SJ.; Anseth, KS. Photopolymerization of hydrogel scaffolds. In: Ma, PX.; Elisseeff, J., editors. *Scaffolding in Tissue Engineering*. Marcel Dekker, Inc.; 2005. p. 69-88.
25. Johnson PM, Reynolds TB, Stansbury JW, Bowman CN. High throughput kinetic analysis of photopolymer conversion using composition and exposure time gradients. *Polymer* 2005;46:3300–6.
26. Domke J, Radmacher M. Measuring the elastic properties of thin polymer films with the atomic force microscope. *Langmuir* 1998;14:3320–5.
27. Wang M, Hill RJ. Electric-field-induced displacement of charged spherical colloids in compressible hydrogels. *Soft Matter* 2008;4:1048–58.
28. Johnson CM, Hanson MN, Helgeson SC. Porcine Cardiac Valvular Subendothelial Cells In Culture - Cell Isolation And Growth-Characteristics. *Journal Of Molecular And Cellular Cardiology* 1987;19:1185–93. [PubMed: 3327949]
29. Rice NA, Leinwand LA. Skeletal myosin heavy chain function in cultured lung myofibroblasts. *Journal of Cell Biology* 2003;163:119–29. [PubMed: 14557251]
30. Rabkin E, Aikawa M, Stone JR, Fukumoto Y, Libby P, Schoen FJ. Activated interstitial myofibroblasts express catabolic enzymes and mediate matrix remodeling in myxomatous heart valves. *Circulation* 2001;104:2525–32. [PubMed: 11714645]



31. Bryant SJ, Nuttelman CR, Anseth KS. Cytocompatibility of UV and visible light photoinitiating systems on cultured NIH/3T3 fibroblasts in vitro. *J Biomater Sci-Polym Ed* 2000;11:439–57. [PubMed: 10896041]
32. Grinnell F. Fibroblasts, Myofibroblasts, and Wound Contraction. *J Cell Biol* 1994;124:401–4. [PubMed: 8106541]
33. Tomasek JJ, Gabbiani G, Hinz B, Chaponnier C, Brown RA. Myofibroblasts and mechano-regulation of connective tissue remodelling. *Nat Rev Mol Cell Biol* 2002;3:349–63. [PubMed: 11988769]
34. Walker GA, Masters KS, Shah DN, Anseth KS, Leinwand LA. Valvular myofibroblast activation by transforming growth factor-beta - Implications for pathological extracellular matrix remodeling in heart valve disease. *CircRes* 2004;95:253–60.
35. Mohler ER. Mechanisms of aortic valve calcification. *Am J Cardiol* 2004;94:1396–402. [PubMed: 15566910]
36. Kaden JJ, Bickelhaupt S, Grobholz R, Vahl CE, Hagl S, Brueckmann M, et al. Expression of bone sialoprotein and bone morphogenetic protein-2 in calcific aortic stenosis. *J Heart Valve Dis* 2004;13:560–6. [PubMed: 15311861]
37. Butcher JT, Nerem RM. Porcine aortic valve interstitial cells in three-dimensional culture: Comparison of phenotype with aortic smooth muscle cells. *J Heart Valve Dis* 2004;13:478–85. [PubMed: 1522296]
38. Cushing MC, Liao JT, Anseth KS. Activation of valvular interstitial cells is mediated by transforming growth factor-beta 1 interactions with matrix molecules. *Matrix Biol* 2005;24:428–37. [PubMed: 16055320]
39. Benton JA, Kern HB, Anseth KS. Substrate properties influence calcification in valvular interstitial cell culture. *The Journal of Heart Valve Disease* 2008;17:689–99. [PubMed: 19137803]

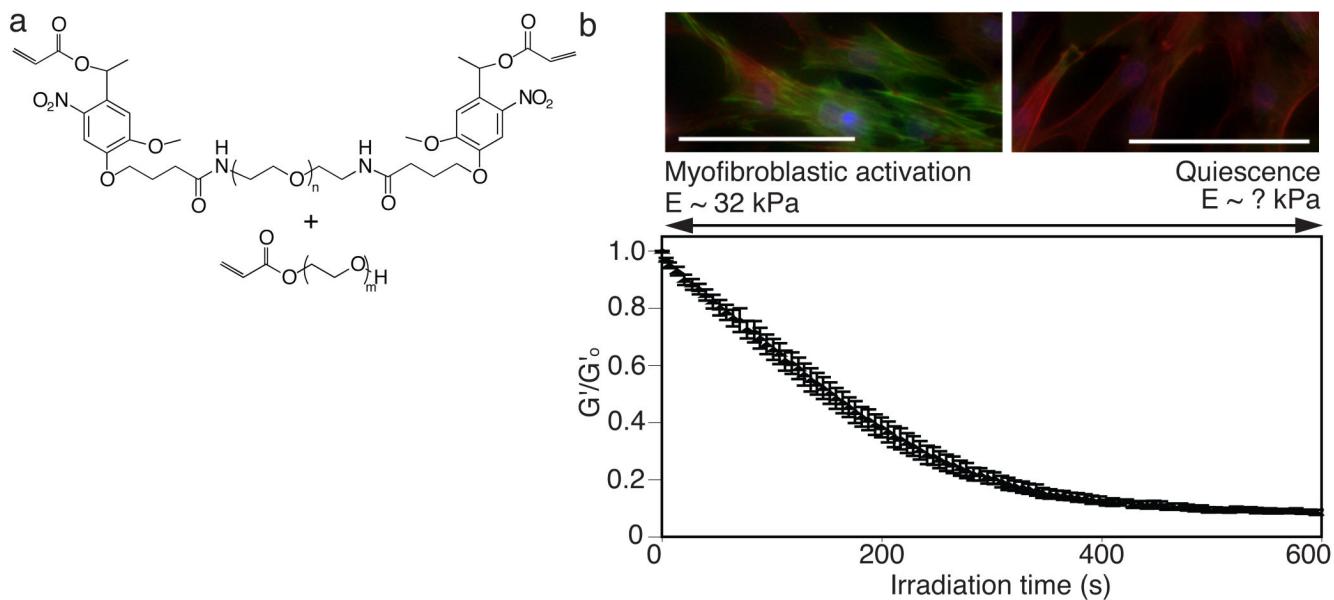


### Figure 1. Hydrogel preparation and characterization

(a) Photodegradable hydrogels were synthesized by redox-initiated radical chain copolymerization of a PEGA (bottom, 6.8 wt%) with PEGdiPDA (top, 8.2 wt%) in PBS. The PEG-based crosslinking macromer contains two nitrobenzyl ether photolabile groups that cleave upon irradiation, releasing PEG and decreasing the modulus of the hydrogel. (b) Degradation was characterized with rheometry, where a thin hydrogel was irradiated *in situ* (365 nm at 10 mW/cm<sup>2</sup>), and the decrease in its elasticity was monitored (storage modulus  $G'$  normalized to initial value  $G'_0 = 10.6$  kPa, Young's modulus ( $E$ )  $\sim 32$  kPa). The elasticity of the hydrogel can be tuned to any of these moduli by irradiation for the corresponding time prior to complete hydrogel degradation,  $\sim 10$  min. These substrates with tunable elasticity can then be used to investigate a range of moduli and to identify substrate moduli that promote (left image) or suppress (right image) VIC myofibroblastic activation ( $\alpha$ SMA green, nuclei blue, and f-actin red). Scale bars, 100  $\mu$ m.

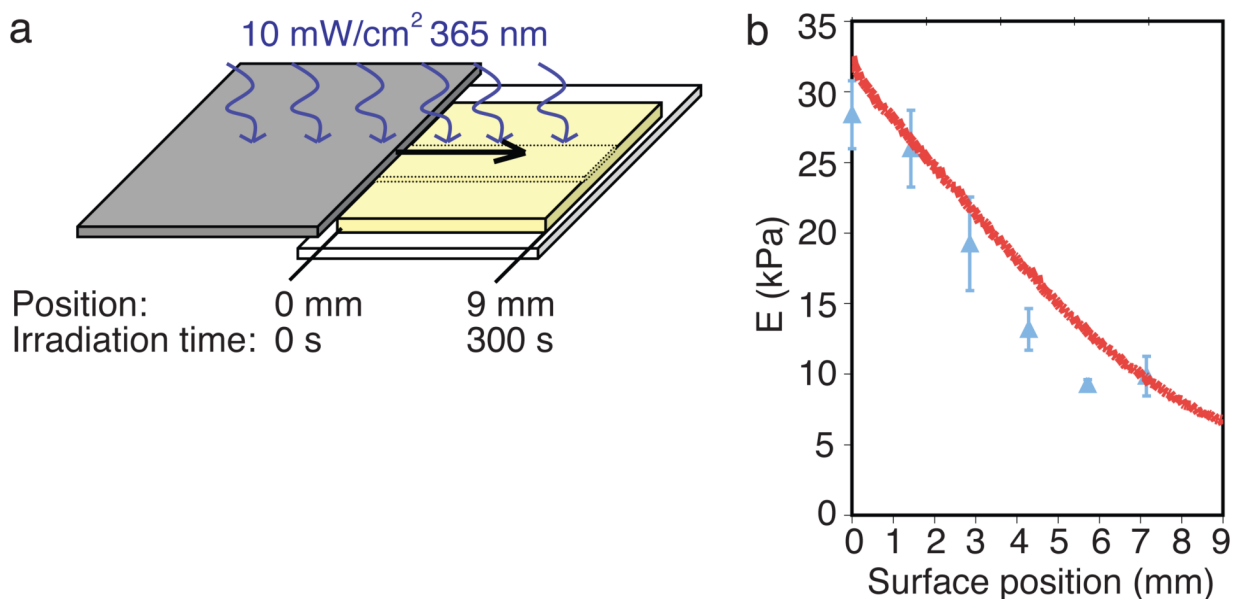


**Figure 2. Cell culture substrate preparation, degradation, and characterization**

**(a)** Exploiting this tunable degradation, hydrogel films were irradiated while covering the film from left to right with an opaque plate to create a linear exposure gradient across the hydrogel (9 mm × 9 mm × 0.25 mm). The left side of the hydrogel received no irradiation, the right side received 5 min of irradiation, and a continuous gradient of irradiation was achieved in between these two extremes (left). This exposure pattern generates an elasticity gradient across the hydrogel surface, the top ~ 50 μm of the gel, corresponding to the elasticity profile observed with rheometry. **(b)** Young's modulus ( $E$ ) was measured at points across the hydrogel with AFM (blue triangles). The moduli across the hydrogel compare well to rheometric measurements at corresponding irradiation times (red line,  $G'$  converted to  $E$  using rubber elasticity theory) and confirm the creation of an elasticity gradient. This gradient spans  $E \sim 32$  kPa to 7 kPa across the surface, moduli similar to that of soft tissues from collagenous bone to muscle [4].

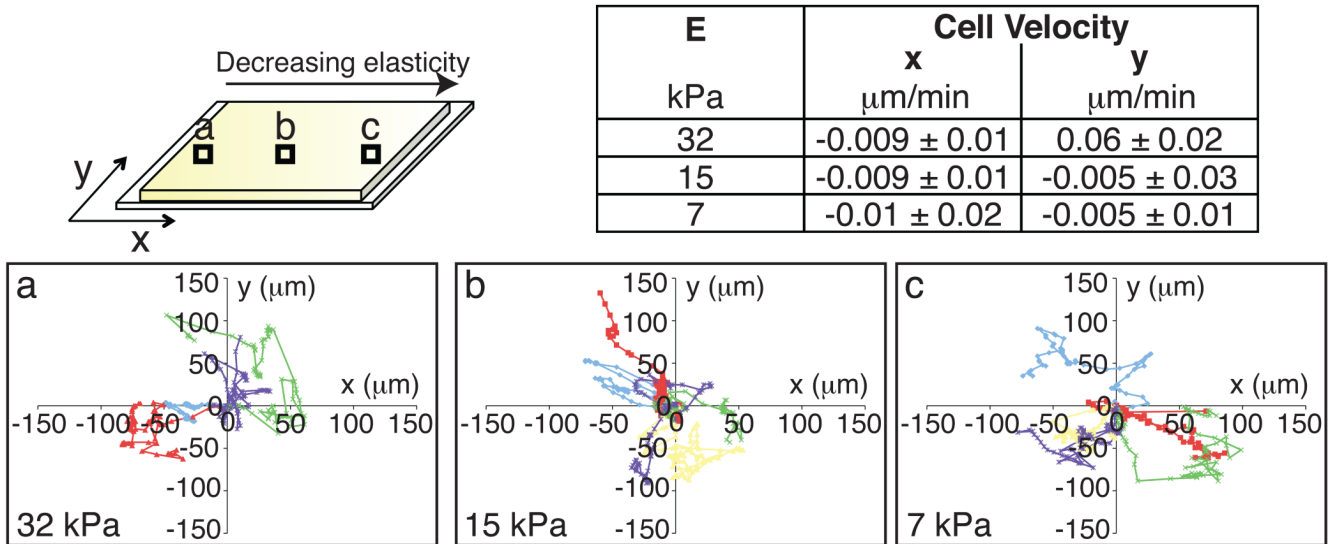


### Figure 3. Cell movement on the elasticity gradient

Cell migration at different positions along the elasticity gradient (32, 15, and 7 kPa) was monitored in real time over 3 days (15 min intervals). Cell velocities in the x and y direction on each elasticity include 0 μm/min, indicating that there was no specific direction in which the cells were traveling (i.e., no directional migration) (table). In addition, no statistical difference was observed between the x or y velocities for these elasticity regions ( $p < 0.9$ ), indicating that cell movement at each position is similar. The movement of several cells was tracked at positions corresponding to different moduli, and corresponding traces of their movement reveal that cells sample many x-y positions but do not move in any specific direction along the gradient nor great distances ( $< 100$  μm on average over 3 days,  $\sim 0.3$  kPa change over 100 μm).

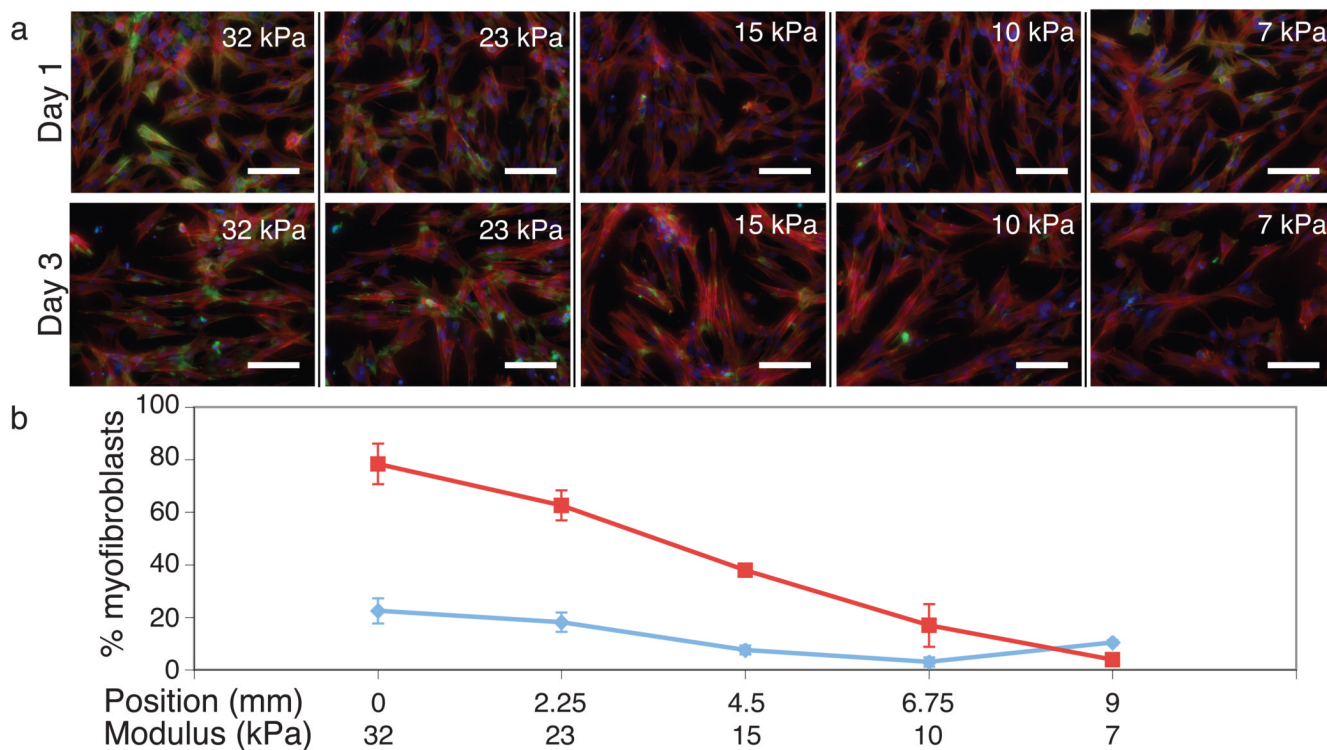


**Figure 4. Cell differentiation on gradient elasticity hydrogels**

(a) VICs cultured on elasticity gradient hydrogels were immunostained for  $\alpha$ SMA (green), an indicator of differentiation to myofibroblasts, as well as f-actin (red) and nuclei (blue). Images were taken at different representative positions along the gradient (moduli noted on image). On Day 1, diffuse  $\alpha$ SMA was present in more cells on the high modulus region of the gradient but not organized. By Day 3,  $\alpha$ SMA was prominent in cells on the high modulus side of the gradient and was organized into stress fibers, indicating myofibroblastic differentiation. (b) To quantify the amount of activated cells, the myofibroblasts at each position on the gel were counted, where increased activation was observed on the high modulus regions of the gradient as compared to the low modulus regions of the gradient on Day 1 (blue diamonds) and Day 3 (red squares). Scale bars, 100  $\mu$ m.



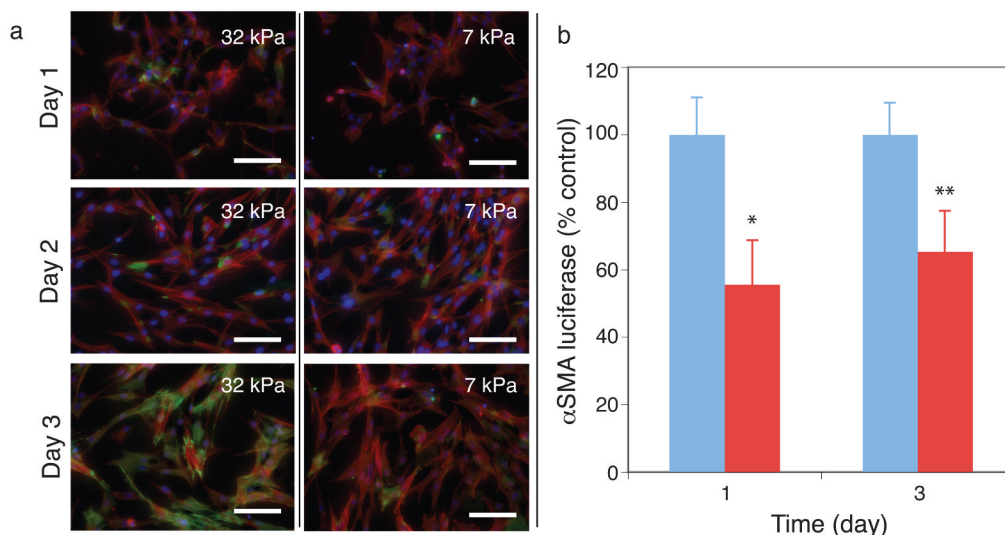


**Figure 5. Cell differentiation on discrete moduli extremes**

(a) To confirm promotion or suppression of differentiation on the two modulus extremes of the gradient,  $E \sim 32$  kPa and 7 kPa, VICs were seeded on discrete high and low modulus samples. On Day 1 and Day 2, some diffuse  $\alpha$ SMA was present but not organized. By Day 3, organized  $\alpha$ SMA stress fibers were prominent on high modulus samples, and limited  $\alpha$ SMA was present on low modulus samples. (b) A luciferase reporter gene expression assay for  $\alpha$ SMA was quantified on these substrates and showed a statistical decrease in  $\alpha$ SMA on low modulus substrates as compared to high modulus substrates (blue 32 kPa, red 7 kPa, measured in relative light units and normalized to high modulus substrate expression (control) at each time, \*  $p < 0.001$  and \*\*  $p < 0.009$ ). These results confirm the promotion and suppression of myofibroblastic differentiation by high modulus and low modulus substrates, respectively. As a whole, this study indicates that substrate elasticity similar to collagenous bone [4] promotes the differentiation of VICs to myofibroblasts, while elasticity similar to muscle [4] suppresses myofibroblastic differentiation. Scale bars, 100  $\mu$ m.

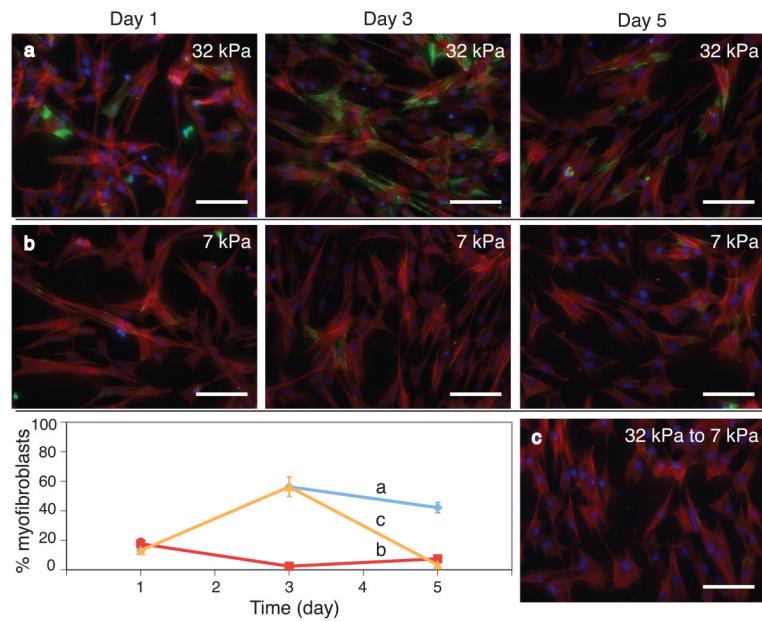


**Figure 6. Modulation of substrate elasticity *in situ* directs myofibroblast de-activation** VICs were cultured on myofibroblast promoting or suppressing substrates for 5 days and immunostained to assess activation: (a) 32 kPa and (b) 7 kPa. On Day 3, a portion of the 32 kPa substrates with activated cells were irradiated for 5 min, decreasing the substrate modulus. By Day 5, almost all cells were de-activated by this *in situ* modulus change ((c) 32 to 7 kPa on Day 3), with a similar number of myofibroblasts present on substrates with a modulus of 7 kPa for the full 5 days. Modulation of substrate elasticity in dynamic cellular processes such as this can lead to a better understanding of its influence on cell function. Scale bars, 100  $\mu$ m.